HHS Public Access

Author manuscript

Cell Rep. Author manuscript; available in PMC 2016 October 12.

Published in final edited form as:

Cell Rep. 2016 September 20; 16(12): 3322–3333. doi:10.1016/j.celrep.2016.08.044.

Neuronal Nuclear Membrane Budding Occurs During a Developmental Window Modulated by Torsin Paralogs

Lauren M. Tanabe[1,*], **Chun-Chi Liang**[1,*], and **William T. Dauer**[1,2]

[1]Department of Neurology, University of Michigan, Ann Arbor, MI 48109, United States

[2]Department of Cell and Developmental Biology, University of Michigan, Ann Arbor, MI 48109, United States

SUMMARY

DYT1 dystonia is a neurodevelopmental disease that manifests during a discrete period of childhood. The disease is caused by impaired function of torsinA, a protein linked to nuclear membrane budding. The relationship of NE budding to neural development and CNS function is unclear, however, obscuring its potential role in dystonia pathogenesis. We find NE budding begins and resolves during a discrete neurodevelopmental window in torsinA null neurons *in vivo*. The developmental resolution of NE budding corresponds to increased torsinB protein, while ablating torsinB from torsinA null neurons prevents budding resolution and causes lethal neural dysfunction. Developmental changes in torsinB also correlate with NE bud formation in differentiating DYT1 embryonic stem cells, and overexpression of torsinA or torsinB rescues NE bud formation in this system. These findings identify a torsinA neurodevelopmental window that is essential for normal CNS function, and have important implications for dystonia pathogenesis and therapeutics.

Graphical abstract

Corresponding Author: William T. Dauer (dauer@med.umich.edu).

*Contributed equally to this work

AUTHOR CONTRIBUTIONS

Lauren M. Tanabe, Chun-Chi Liang, and William T. Dauer designed the experiments and wrote the paper. Lauren M. Tanabe and Chun-Chi Liang conducted experiments.

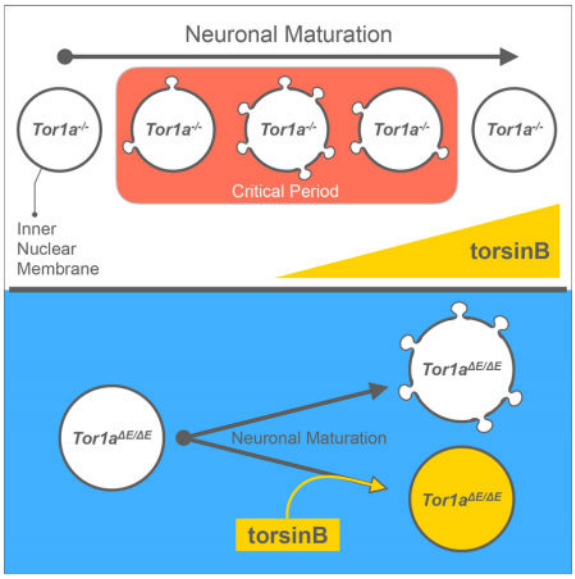

INTRODUCTION

An important challenge to unraveling the pathogenesis of inherited neurodevelopmental diseases is determining whether pathogenic proteins play unique roles during CNS development (e.g., during a neurodevelopmental window). This challenge is exemplified by torsinA, a AAA+ protein that causes DYT1 dystonia when its gene is mutated. The abnormal twisting movements that characterize DYT1 dystonia emerge during a discrete period of childhood, but mutation carriers who do not manifest dystonia during this window, typically remain symptom free for life. Determining whether there is a unique temporal requirement for normal torsinA function during CNS development is essential for the identification of key pathophysiological events, accurate disease modeling, and targeted therapeutic development.

The DYT1 mutation is a 3-bp in-frame deletion in *TOR1A*, which removes a single glutamic acid residue (“ΔE”) from torsinA (Ozelius et al., 1997). TorsinA is a membrane-associated protein that resides within the endoplasmic reticulum (ER)/nuclear envelope (NE) endomembrane space. Several observations support a normal role for torsinA at the NE that is disrupted by the DYT1 mutation. An engineered mutation that blocks torsinA ATP hydrolysis also causes the protein to accumulate abnormally in the perinuclear space (Gonzalez-Alegre and Paulson, 2004; Goodchild and Dauer, 2004; Naismith et al., 2004). Wild type torsinA interacts with the NE proteins lamina-associated polypeptide 1 (LAP1), SUN1, and several nesprins (Goodchild et al., 2005; Jungwirth et al., 2011; Nery et al., 2008). LAP1 forms a hetero-oligomer with torsinA and is essential for its enzymatic (ATPase) activity (Brown et al., 2014; Sosa et al., 2014; Zhao et al., 2013). The DYT1 mutation impairs binding of torsinA to LAP1 and causes torsinA to accumulate abnormally within the perinuclear space, a phenomenon that requires SUN1 (Jungwirth et al., 2011; Naismith et al., 2009; Zhao et al., 2013). The relevance of these events to dystonia is

supported by the finding that a mutation in LAP1 causes a severe form of childhood dystonia (Dorboz et al., 2014).

Mouse genetic experiments provide strong *in vivo* support for a potential link between torsinA activity, nuclear membrane function, and dystonic movements. These experiments demonstrate that the DYT1 mutation impairs torsinA function, causing abnormal twisting movements and striking morphological abnormalities of the nuclear membrane selectively in post-migratory neurons (Goodchild et al., 2005; Liang et al., 2014; Weisheit and Dauer, 2015). These nuclear abnormalities are membranous out-pouchings (termed “buds”) that emerge from the inner nuclear membrane and protrude into the perinuclear space. The exclusive appearance of buds in neurons and their apparent relationship to neuronal maturation are consistent with a role for nuclear membrane dysfunction in the pathogenesis of DYT1 dystonia (Goodchild et al., 2005; Liang et al., 2014; Weisheit and Dauer, 2015).

Structures similar to neuronal NE buds have been observed in several developmental contexts in diverse wild type organisms (Clark, 1960; Hadek and Swift, 1962; Hochstrasser and Sedat, 1987a; D. Szöllösi, 1965; M. S. Szöllösi and D. Szöllösi, 1988). Some observations indicate that these buds may represent structural intermediates of a poorly understood form of nuclear pore-independent nucleo-cytosolic transport, a process possibly analogous to herpesvirus nuclear egress (Maric et al., 2014). In *Drosophila*, bud-like structures are implicated in the normal transport of “mega” ribonucleoprotein complexes containing Wingless signaling components (e.g., the C-terminal cleavage product of DFrizzled-2) across the post-synaptic nuclear membrane (Speese et al., 2012). *Drosophila* torsin protein appears localized to the necks of these structures, and *Drosophila* torsin mutants show defects in transport of mRNAs contained within the vesicles, and related abnormalities of neuromuscular junction development (Jokhi et al., 2013).

The observation of similar nuclear membrane out-pouchings in early developmental contexts has led to the suggestion that this process may be required specifically when bursts of coordinated protein synthesis are required to support critically timed differentiation or maturation events (Strambio-De-Castilla, 2013). Indeed, buds in the neuronal nuclei of torsinA null (or homozygous DYT1 ΔE knock-in) mice appear selectively in post-migratory maturing neurons (Goodchild et al., 2005), cells highly utilizing the machinery of mRNA synthesis and transport. Other work links torsinA loss-of-function to abnormalities of nuclear pore biogenesis and function (VanGompel et al., 2015), suggesting that the dramatic increase in neuronal nuclear pore number in maturing neurons (Lodin et al., 1978) may also contribute to NE budding. These mechanisms imply a relationship between bud formation and CNS maturation. It has not been possible to explore this question directly, however, because of the perinatal lethality of torsinA mutant mice, and absence of an *in vitro* model of this process (Goodchild et al., 2005; Liang et al., 2014; Tanabe et al., 2012).

Here, we demonstrate that neuronal nuclear membrane budding is a developmentally regulated event and identify a molecular component of this process that controls its timing. Neuronal NE budding in torsin mutant neurons occurs initially following neuronal migration, and peaks during a period corresponding to synaptic integration and circuit formation. Remarkably, NE buds then disappear completely as neurons fully mature. This

developmental window is strongly modulated by the torsinA paralog, torsinB. The developmental upregulation of endogenous torsinB levels corresponds to the disappearance of buds, and in mice null for both torsinA and torsinB, NE buds develop earlier (in migrating neurons) and persist into adulthood. We model this process *in vitro* during the neural specification of DYT1 mutant mouse ES (mES) cells, and demonstrate that overexpression of torsinB (or torsinA) can rescue NE bud formation. These findings link neuronal NE budding to a discrete neurodevelopmental window, provide molecular insight into this process, and have important implications for understanding the pathogenesis of DYT1 dystonia.

EXPERIMENTAL PROCEDURES

Mouse Breeding and Genotyping

Animal testing was conducted in accord with the National Institutes of Health laboratory animal care guidelines and with the Institutional Animal Care and Use Committee at the University of Michigan. Prenatal birthdating of mice was determined by the presence of a vaginal plug, designated as embryonic day 0.5 (E 0.5). For postnatal birthdating, the day of birth was designated as P0. Nestin-*Cre*, Synapsin 1-*Cre*, and Dlx5/6-*Cre* mice were obtained from The Jackson Laboratory. *Tor1a* floxed mice were described previously (Liang et al., 2014). *Tor1b* floxed mice were generated by introducing LoxP sites in the *Tor1b* introns in between exons 2 and 3 and after exon 5 (Fig. S3). *Tor1(ab)* floxed animals contain LoxP sites in the *Tor1a* intron between exons 2 and 3, and the *Tor1b* intron between exons 2 and 3 (Fig. 3). Both *Tor1b* and *Tor1(ab)* floxed mice are generated by the standard method, as described previously (Liang et al., 2014). Mouse genotyping and breeding is described in detail in Supplemental Experimental Procedures.

Generation of mES Cell Clones

The $Tor1a^{+/+}$ and $Tor1a^{\Delta E/\Delta E}$ mES cell lines were generated by superovulating $Tor1a^{\Delta E/+}$ female mice, and mating them with $Tor1a^{\Delta E/+}$ male mice. At 3.5 dpc, blastocysts were flushed from the ovaries of female mice that displayed vaginal plugs. Blastocysts were plated on a mitomycin-C treated mouse embryonic fibroblast (MEF) feeder layer. During the next 4 days blastocysts hatched and attached to the plate. More MEFs were added on day 4 of plating. The following day and everyday after that, cells were fed with fresh ES medium containing a Mek1/2 inhibitor (U0126; Cell Signaling Technology) until ES colonies were observed and plentiful. At day 8 and every few days after that the well was trypsinized and passed to another well with an established feeder layer for each blastocyst. This was done repeatedly and the clones were expanded to a 10-cm plate and frozen down.

mES Cell Culture and *in vitro* Differentiation

Neural Lineage—Mouse embryonic stem cells (mES) were plated and maintained for two passages on treated tissue culture plates coated with 0.1% gelatin and mitotically inactivated mouse embryonic fibroblast (MEF) cells, followed by two additional passages on gelatin coated plates without MEF feeders (Millipore) in ES medium (DMEM with 4500 mg/l glucose and 2250 mg/l Na-bicarbonate supplemented with 1X nonessential amino acids, 1X nucleosides (Specialty Media), 0.1 mM β-mercaptoethanol (Sigma), 2 mM L-glutamine

(GIBCO), Penicillin/Streptomycin (GIBCO), 15% FBS (HyClone), and 1000 units/ml LIF (Chemicon). Prior to differentiation, mES cells were trypsinized, dissociated, and plated as single cells in suspension (2.0×10^6 cells in 15 mL serum free differentiation medium). These cells were grown in aggregate cultures for 2 days to form embryoid bodies (EBs) in serum-free medium (Advanced DMEM/F12 (Gibco) and Neurobasal (Gibco) media in a 1:1 ratio supplemented with Knock-Out Serum Replacement (10% by volume; Invitrogen), penicillin/streptomycin (1.0% by volume; Sigma), L-glutamine (200 mM), and β-mercaptoethanol (0.1 mM; Sigma). Following 2 days in suspension culture, EBs were split 1:2 and treated with retinoic acid (RA; Sigma) dissolved in dimethyl-sulfoxide (1 μM; Sigma; 0.1% of total volume). EBs were cultured for a total of 5 days in RA-containing medium. They were then transferred to PDL/laminin (Sigma) coated plates in non-RA containing maturation medium (Advanced DMEM/F12 and Neurobasal media, B27 supplement (2.5% by volume; Invitrogen), L-glutamine (200 μM), penicillin/streptomycin (1.0% by volume).

Cardiomyocyte Lineage—Following EB formation (48 hrs), EBs were split 1:2 and replated in suspension culture plates in the same media described above, except with 10% FBS and the addition of 0.1 mg/mL ascorbic acid (Sigma). EBs were exposed to this formulation for 5 days. EBs were then transferred to gelatin-coated tissue culture treated plates in the same media as used for differentiation except without 0.1 mg/mL ascorbic acid. EBs adhered to plates after 24 hrs and beating foci were detected after 48 hrs.

Protein Extraction from Tissue and Cells and Western blotting

For tissue extraction, animals were heavily anesthetized with ketamine and xylazine, ip, and transcardially perfused with ice cold PBS. Tissue was lysed by sonicating with 1.0% SDS lysis buffer containing 100 mM Tris-HCl (pH 8.0), 10% glycerol, 150 mM NaCl, 2 mM EDTA, and protease inhibitor cocktail (Sigma). Protein concentration was determined with BCA assay (Pierce). Proteins were denatured prior to SDS-PAGE by boiling with Laemmli's sample buffer (Bio-rad) containing β-mercaptoethanol for 5 minutes. After SDS-PAGE, proteins were transferred to nitrocellulose membrane, which was blocked with blocking buffer (5.0% skim milk in PBS with 0.2% Tween) for 1 hour at room temperature. Blocked membrane was incubated in blocking buffer containing primary antibody overnight at 4 °C. Membrane was washed with washing buffer (PBS with 0.2% Tween; PBS-T) and then incubated in blocking buffer with HRP-conjugated secondary antibody for 1 hour at room temperature. The washed membrane was developed using chemiluminescent substrate for HRP (Pierce) and exposed on film (Kodak X-omat LS films or Amersham Hyperfilm). All western blots were quantified with densitometry using ImageJ. All levels were calculated relative to calnexin loading control.

Antibodies

The dilution rates for each antibody used in this study are listed as follows. anti-torsinA (rabbit polyclonal, Abcam; 1:10,000); anti-torsinB (rabbit polyclonal; kind gifts of Dr. Rose Goodchild; VIB Center for the Biology of Disease and Dr. Christian Schlieker, Yale University; 1:1000); anti-LAP1 and anti-LULL1 (rabbit polyclonal; kind gift of Dr. Christian Schlieker; Yale University; 1:1000); anti-calnexin (rabbit polyclonal, Stressgen;

1:10,000); anti GAD65/67 (rabbit polyclonal, Millipore; 1:2000); anti-neurofilament-M (rabbit polyclonal, Millipore; 1:200); γ-tubulin (monoclonal, Sigma; 1:2000); anti-NeuN (Monoclonal A-60, Millipore; 1:200); anti-GABA (rabbit polyclonal, Sigma, 1:200); anti-GFP (rabbit polyclonal, Abcam; 1:200); Goat anti-Rabbit IgG Horse Radish Peroxidase and Goat anti-Mouse IgG Horse Radish Peroxidase (Cell signaling; 1:10,000); anti-mouse Alexa Fluor 488, anti-rabbit Alexa Fluor 488, and anti-rabbit Alexa Fluor 633 (Invitrogen; 1:400).

Statistics

GraphPad Prism software (GraphPad Software, Inc.) was used to analyze all data. Means are displayed with error bars representing SEM. One-way ANOVA tests were followed by post hoc Dunnett test, where appropriate. Mouse survival probability was analyzed using the Kaplan and Meier method. Analyses of NE buds quantification for the control condition of wild-type mice is not included because we never observe NE budding in wild type tissue or cells, as initially reported (Goodchild et al., 2005), and confirmed in extensive experiments since (Kim et al., 2010; Weisheit and Dauer, 2015). Similarly, we never observe NE buds in wild type ES cells driven down a neural lineage.

RESULTS

Neuronal Nuclear Envelope Budding is a Cell Autonomous Process That Occurs during a Discrete Neurodevelopmental Window

Perinatal lethality of constitutive torsinA null mice has limited our understanding of the relationship between CNS maturation and NE budding. We reported recently that conditional deletion of torsinA from the CNS (using nestin-*Cre*; "N-CKO" mice) is compatible with life for up to 16 days of age (Liang et al., 2014), enabling us to advance understanding of this question. We first confirmed that deletion of torsinA from neural progenitor cells (the stage of nestin-*Cre* expression) caused nuclear buds indistinguishable from those previously reported in constitutive null and DYT1 knock-in mice (Goodchild et al., 2005; Tanabe et al., 2012) (Fig. 1A). To explore the relationship between NE budding and CNS maturation, we quantified the percentage of neurons with NE buds in several brain regions on the day of birth (P0) and in the more mature CNS (P8). All brain regions examined developed NE buds (Fig. 1A–B; Fig. S1), and the developmental age of the brain region strongly influenced the percentage of affected neurons observed (Fig. 1B–E). At P0, earlier maturing caudal regions such as spinal cord and brainstem (pons) contained a considerably higher percentages of NE bud-bearing neurons (and NE buds/neuron) than later maturing rostral regions, such as the striatum (Fig. 1B–C). In all regions examined, the percentage of affected neurons (and NE buds/neuron) increased with ongoing CNS maturation (i.e., from P0 to P8; Fig. 1B, D–E). Additionally, the relationship between NE buds and developmental age was observed within brain regions containing neural classes of differing maturational ages. For example, at P8 ~80% of earlier-born Purkinje cells (born ~E12.5) contained NE buds, whereas only ~6% later-born granule cells are affected (birthdate ~E13–E17; postmitotic from P3 onwards; Fig. 1B) (Machold and Fishell, 2005; Mizuhara et al., 2010). Considered together with our previous findings, these observations indicate that NE bud formation, which begins following neuronal migration (Goodchild et al., 2005), continues during postnatal CNS maturation.

Little is understood about the cellular or molecular requirements for neuronal NE budding. To examine whether NE bud formation is a neural cell autonomous process, we deleted torsinA selectively from neurons by intercrossing floxed torsinA and Synapsin 1-*Cre* transgenic mice (herein Syn-CKO mice). The Synapsin 1-*Cre* transgene begins to express in maturing neurons, as early as ~E12.5 (Zhu et al., 2001). Syn-CKO mice showed near complete deletion of torsinA in the spinal cord and brainstem, efficient deletion in cortex, and little or no deletion in cerebellum and striatum, a pattern corresponding to transgene expression (Fig. 2A–B and Fig. S2A). All regions showing efficient torsinA deletion developed NE buds indistinguishable from those seen in N-CKO mice (Fig. 2C; Fig. S2B), demonstrating that NE budding is a neuronal cell autonomous process.

To examine the developmental dependence of NE budding during the complete process of neural maturation, we examined multiple ages in the striata of Dlx5/6-*Cre* conditional torsinA mutants that live into adulthood (herein Dlx5/6 conditional KO “Dlx-CKO”; Pappas et al., 2015). Additional advantages of this model are the relative homogeneity of the striatum (95% of striatal cells are medium spiny neurons) and the strong links between striatal dysfunction and dystonia pathogenesis (Pappas et al., 2015; Tanabe et al., 2012). These mice exhibited essentially complete deletion of torsinA from the striatum (Fig. 2D). Despite early (E12.5) prenatal deletion of torsinA by Dlx-5/6-*Cre* (Monory et al., 2006; Pappas et al., 2015), striatal NE buds did not begin to appear until ~P3. Similar to N-CKO and Syn-CKO mice, NE budding frequency increased during CNS maturation, reaching a peak of ~35% of neurons at ~P7. Surprisingly, the percentage of NE bud-bearing neurons then decreased rapidly during the second postnatal week (P7 – 14), and NE buds were essentially undetectable by P42 (Fig. 2E). This disappearance of NE blebs is not due to cell death, as striatal size and the number of medium spiny neurons are normal in Dlx-CKO mice (Pappas et al., 2015), and assessment by TEM showed no apoptotic nuclei or other ultrastructural evidence of cell toxicity. Similar to Dlx-CKO mice, analysis of older Syn-CKO mice (P23) also demonstrated complete absence of NE buds (Fig. S2 C). These data demonstrate that neuronal NE budding does not continue to progressively increase with age as implied by findings in N-CKO mice (Fig. 1B) and in previous work (Goodchild et al., 2005; Kim et al., 2010). Rather, NE budding is confined to a discrete neurodevelopmental window, implying the existence of factors that modulate this process.

An intriguing candidate as a regulator of NE budding is the torsinA paralog, torsinB. We reported previously that *in vitro* torsinA and torsinB have conserved function at the NE and that in torsinA null tissue, levels of torsinB strongly influence the susceptibility of different cell types to the formation of NE buds (e.g., in neuronal vs. non-neuronal cells) (Kim et al., 2010). Other work demonstrates differential expression of torsinB both spatially and temporally in mouse and human brain (Bahn et al., 2006; Jungwirth et al., 2010; Vasudevan et al., 2006). Therefore, we explored whether physiological changes in the developmental expression of torsinB might correspond to the appearance and disappearance of NE buds in Dlx-CKO mice. Consistent with this notion, we found that in wild type mice, striatal torsinB levels are low during the first postnatal week when NE buds are accumulating, and then increase by more than 3-fold during the second postnatal week coincident with NE bud disappearance (Fig. 2E–G). TorsinA levels show the converse pattern, decreasing after the first postnatal week (Fig 2F–G). Levels of torsinA interacting proteins LAP1 and LULL1

remain largely unchanged in this time frame (Fig. 2F–G). These observations implicate torsinB in the developmental regulation of neuronal NE budding, and suggest a potential molecular mechanism underlying the selective vulnerability of immature neurons to torsinA loss of function.

TorsinB Modulates the Developmental Dependence of Neuronal NE Budding

To investigate directly a role for torsinB in neuronal NE budding, we used gene targeting to explore the consequences of *Tor1b* deletion, and the effect of altering torsinB function in the context of torsinA loss-of-function (Fig. S3). Intercrossing germline $Tor1b^{+/-}$ mice generated all expected genotypes at normal Mendelian frequency. $Tor1b^{-/-}$ mice were indistinguishable from their littermate controls and showed no NE buds in the CNS or peripheral tissues (including heart, tongue, liver and kidney; data not shown). *Tor1a* and *Tor1b* are adjacently located, precluding the possibility of intercrossing the individual mutant alleles to create torsinA and torsinB double null mice. We therefore generated a floxed allele in which the LoxP sites encompass *both Tor1a* and *Tor1b* (Fig. 3A). No germline torsinA/torsinB **d**ouble **K**nock **O**ut mice ($Tor1(ab)^{-/-}$ or "dKO") were recovered from the litters of $Tor1(ab)^{+/-}$ intercrosses. Assessment of prenatal time points demonstrated that germline dKO embryos developmentally arrest at ~E8.5 (data not shown). Considering the lack of phenotype in $Tor1b^{-/-}$ mice, this finding is consistent with previous work indicating that torsinA and torsinB share conserved function (Kim et al., 2010).

To overcome the embryonic lethality of dKO mice and examine a potential role for torsinB in modifying torsinA-related NE budding, we used nestin-*Cre* to conditionally delete these genes from neural progenitor cells (**n**estin **d**ouble **c**onditional **k**nock **o**ut, herein "N-dCKO"; Fig. 3B). N-dCKO mice were recovered at reduced Mendelian ratios in newborn litters, but at normal Mendelian ratios at E16.5, indicating that many die during late gestation (Table S1). All N-dCKO mice identified in newborn litters died in the first 12 hours of life. Standard histological analysis (e.g., Nissl and H & E staining) of the brains of these mice did not reveal any gross abnormalities (data not shown).

In striking contrast to the neurodevelopmental dependence of NE buds observed in N-CKO mice (Fig. 1B), essentially all N-dCKO neurons exhibited NE buds, regardless of maturational state (Fig. 3C–H). N-dCKO nuclei (Fig. 3D) also exhibited greater numbers of buds than N-CKO nuclei (Fig. 1C). Strikingly, NE buds were also observed in N-dCKO migrating neurons (Fig. 3E–H), a developmental stage at which NE buds are never seen in N-CKO (data not shown) or *Tor1a* null or ΔE-torsinA knock-in mice (Goodchild et al., 2005). This observation suggests that torsinB participates in timing of initiation of NE budding during neurodevelopment.

To determine whether the later increase in torsinB levels (Fig. 2F–G) might likewise be involved in the developmental downregulation of NE budding, we examined a role for this protein in later maturing neurons. This question could not be addressed in N-dCKO (Table S1) or Dlx-dCKO (Fig. S4A) mice because of the early lethality in these lines. We therefore utilized Synapsin 1-*Cre*. Mice in which both torsinA and torsinB were deleted using Synapsin 1-*Cre* ("Syn-dCKO") (Fig. 4A) were born in normal Mendelian ratios and survived for up to 6 weeks (median age = 23 days, Fig. S4B). Whereas NE buds are absent by P23 in

Syn-CKO mice (Fig. S2C), NE buds remain or continue to increase in all structures examined in Syn-dCKO animals (Fig. 4B–C). Importantly, the early lethality of Syn-dCKO mice – in which deletion is exclusively neuronal – link dysregulation of NE-budding to neuronal dysfunction. Considered together, these data identify torsinB as a regulator of the opening and closing of the neurodevelopmental window for NE budding in torsinA mutant mice.

A DYT1 Mutant ES Cell Model Recapitulates Neurodevelopmental Onset of NE Budding and Provides a Platform for Molecular Therapeutics

Having established *in vivo* an essential role for torsinB in the *closing* of the NE budding window (Fig. 4B), we next pursued a series of experiments to further explore the role of torsinB during the *opening* of the NE budding window. Critically, we sought to explore whether overexpression torsinA or torsinB could “rescue” NE budding. In an attempt to translate our findings into a more disease-relevant context, we pursued these studies in the context of ΔE-torsinA (as exists in DYT1 dystonia subjects). Neuronal NE budding of $Tor1a^{\Delta E/\Delta E}$ mice is indistinguishable from that of torsinA null mice and NE buds are not observed in $Tor1a^{+/+}$ or $Tor1a^{\Delta E/+}$ littermate controls (Goodchild et al., 2005). We therefore derived multiple independent mouse embryonic stem cell (mES) lines from an allelic series of ΔE-torsinA knock-in mice. To test whether neuronal differentiation of the mES clones replicates a maturation-related budding phenomenon selectively in neurons, we drove $Tor1a^{+/+}$ and $Tor1a^{\Delta E/\Delta E}$ mES clones down either the neuronal or cardiomyocyte lineages (Fig. 5A). We utilized a paradigm in which the mES were differentiated into embryoid bodies (EB), treated with either retinoic acid (neural lineage) or ascorbic acid (cardiomyocyte lineage), and subsequently plated onto an appropriate substrate for further maturation (PDL/laminin for neurons or gelatin for cardiomyocytes; Fig. 5A). No differences in maturation were observed between $Tor1a^{+/+}$ and $Tor1a^{\Delta E/\Delta E}$ when driven down either lineage. After 5 days of RA exposure, both genotypes differentiated into GABAergic neurons expressing medium chain neurofilament and GAD65/67 (Fig. 5B) and developed extensive neuronal processes following plating onto PDL/laminin. Similarly, cultures of both genotypes developed foci of contracting cells ~2 days following ascorbic acid exposure (Video S1). *In vivo*, NE buds emerge selectively in post-migratory maturing neurons (Goodchild et al., 2005) and increase during neuronal maturation (Fig. 1 and 2). We observed a similar pattern of NE bud development during *in vitro* neuronal differentiation: $Tor1a^{\Delta E/\Delta E}$ neuronal EBs developed NE buds that were morphologically indistinguishable from those observed *in vivo* (Fig. 5C), and the percentage of affected cells increased with neural maturation (Fig. 5D; Day 5 ~ 5%; Day 13 ~ 60%). Similar to the neural specificity of NE buds *in vivo*, no nuclear buds were observed when $Tor1a^{\Delta E/\Delta E}$ ES cells were driven down the cardiomyocyte lineage (Fig. 5C). Strikingly, opposite patterns of torsinB expression were observed in these two lineages. TorsinB levels decreased during neural differentiation but increased during cardiomyocyte differentiation (Fig. 5E–F), establishing another context in which levels of torsinB anti-correlate with the formation of NE buds. These data demonstrate that the mES differentiation paradigms recapitulate fundamental attributes of torsinA-associated NE budding seen *in vivo:* neuronal cell specificity and autonomy, developmental dependence, and anti-correlation with levels of torsinB.

Having established this *in vitro* platform, we tested whether increasing levels of torsinB could suppress NE bud formation. This experiment further tests the role of torsinB in NE bud dynamics, and – in the context of ΔE-torsinA – is relevant to the development of DYT1 therapeutics. We transduced EBs with GFP-tagged-torsinA, -torsinB, or -torsin2-expressing lentiviruses on RA-differentiation day 2, when EBs are beginning to acquire neuroprogenitor characteristics (Bain et al., 1996). Both torsinA and torsinB significantly decreased the percentage of nuclei with NE buds (by nearly 50%). Torsin2 had no significant effect (Fig. 5G) but also appeared to potentially reduce NE buds, raising the possibility that other torsin proteins may be involved in this process. Transduction of EBs did not alter the trajectory of neuronal differentiation, as all virally-transduced EBs expressed NeuN and GABA at the same rate (Figs. S5A) and to the same extent as non-transduced EBs, and transduction efficiency was similar among the different torsin isoforms (Figs. S5B). These further support an inverse relationship between torsinB levels and NE bud formation. Considered together, these results establish the utility of this model system for identifying factors that can mitigate or prevent the deleterious effects of torsinA loss-of-function at the NE.

DISCUSSION

Our studies establish a neurodevelopmental window for torsinA-related NE budding during CNS maturation *in vivo*. These data demonstrate that NE budding is a neurodevelopmentally regulated process and to describe the lethal consequences for the organism when it is allowed to continue unabated. A regulated role for NE budding during development is consistent with several previous observations of NE buds in developmental contexts (Gay, 1956; Hadek and Swift, 1962; Hochstrasser and Sedat, 1987b; Speese et al., 2012; M. S. Szöllösi and D. Szöllösi, 1988). Considered together, these observations suggest that NE budding may be a normal cellular process, and the appearance of buds may reflect a stalled structural intermediate, the progression of which is slowed or blocked by the absence of torsinA function. The lethality that occurs when this process is continually dysregulated – including selectively within neurons – support its essential role in CNS function. We also identify torsinB as a potent molecular modifier of torsinA-dependent NE budding, demonstrating its ability to strongly influence both the opening and closing of the neurodevelopmental window for this process, and show that overexpression of torsinB can suppress NE bud formation in an *in vitro* model of DYT1 dystonia. These findings provide a powerful platform for further elucidation of the biological roles of NE budding during neural development, and highlight the importance of studying the developing CNS to identify torsinA processes relevant to the pathogenesis of dystonia.

DYT1 dystonia is ~30% penetrant and essentially no mutation carriers that remain unaffected by their 20’s subsequently develop symptoms. This pattern suggests that pathogenic torsinA is capable of disrupting motor circuits only during an early neurodevelopmental window. We explored this possibility by conditionally deleting torsinA from the murine CNS and analyzing NE budding throughout CNS maturation. Using this approach, we identify a strong relationship between developmental age and susceptibility to torsinA loss-of-function. Whereas previous work implied that NE buds continue to accumulate without end, we now demonstrate that NE buds disappear in all mutant lines that survive into adulthood (Syn-CKO, Dlx-CKO, Fig. 2E, Fig. S2C). Considered together, these

data establish an essential requirement for torsinA function during a neurodevelopmental window during CNS maturation.

Considerable uncertainty exists about the human age that corresponds to the early postnatal stage we identify as critically dependent upon normal torsinA function. This period, however, is likely earlier than the early childhood period when dystonic symptoms emerge in DYT1 subjects. We propose a model whereby early abnormalities of neural circuits consequent to torsinA loss-of-function disrupt the highly dynamic developmental trajectory that occurs throughout childhood, resulting in the later emergence of dystonic symptoms. Consistent with this model, behavioral abnormalities emerge and subsequently worsen when NE buds have largely resolved in Dlx-CKO striatum (Pappas et al., 2015). NE buds peak at P7, yet are largely absent by P14 (Fig 2E). However, Dlx-CKO mice are indistinguishable from littermate controls until P14 when abnormal twisting movements emerge, and progressive abnormalities on the grid hang test do not emerge until P21, and then worsen over the next 2–3 weeks. The concept of early deleterious events causing symptoms to emerge much later, consequent to altered neurodevelopmental trajectories, is well established in studies of autism and schizophrenia, among other neurodevelopmental disorders (Connors et al., 2008; Hoftman and Lewis, 2011; Shaw et al., 2010). Our current findings, previous work identifying other torsinA loss-of-function pathologies confined to early postnatal development (Liang et al., 2014; Pappas et al., 2015; Weisheit and Dauer, 2015), and the clinical phenomenon of delayed-onset dystonia (Burke et al., 1980) suggest that this model of disease pathogenesis may also apply to DYT1 and other childhood-onset primary dystonias.

To provide mechanistic understanding of NE budding and identify therapeutic targets for DYT1 dystonia, we next sought factors that modulate this neurodevelopmental window. We and others have documented marked differences in the levels of torsinB between neural and non-neural tissue that correlate with susceptibility to NE bud formation (Jungwirth et al., 2010; Kim et al., 2010). Data from rodent and human brains indicate that levels of torsinB are low prenatally, and increase substantially thereafter (Bahn et al., 2006; Vasudevan et al., 2006). The timing of increased torsinB expression presented an ideal opportunity to study the relationship of torsinB levels and NE buds in striatum, a structure strongly implicated in dystonia. Consistent with a potential role for torsinB in regulating NE bud dynamics, torsinB levels remain low during the peak of NE bud formation, but increase by ~3-fold coincident with NE bud disappearance (Fig. 2F–G).

To directly test the role of torsinB in NE bud dynamics, we experimentally manipulated torsinB levels in several *in vivo* and *in vitro* contexts. In contrast to the developmental gradient observed in N-CKO mice, nearly all N-dCKO neurons exhibited buds, regardless of developmental age (Fig. 3C–D). Notably, loss of torsinB on the torsinA null background dramatically lengthened the neurodevelopmental window, causing NE buds to form in migrating neurons (Fig. 3E–H) and to persist in mature neurons – maturational states in which NE buds are never seen in torsinA null mice. The neurodevelopmental window failed to close in the absence of torsinB (Figs. 4B–C), causing a progressive increase in NE buds and early lethality. Importantly, Syn-CKO mice show normal viability whereas Syn-dCKO mice die by 6 weeks of age. Markedly earlier lethality was also seen in all other double

knockout mice compared to torsinA deletion alone, strengthening the connection between NE buds and neuronal function. Conversely, we demonstrate that experimentally increasing levels of torsinB can suppress NE bud formation in a novel *in vitro* model of DYT1 dystonia. These data establish the changes during CNS maturation of endogenous torsinB levels as a physiological mechanism modulating the window of vulnerability to torsinA loss of function. Considered with previous work (Kim et. al., 2010, Zhao et.al., 2013), it is most likely that torsinA and torsinB share a redundant function at the NE and that developmental window for NE budding reflects a time when aggregate torsin protein function (represented by the combination of torsinA and torsinB levels) dips below a critical threshold.

The ability of torsinA or torsinB to suppress NE budding in immature neurons contrasts with our previous work (Kim et al., 2010) demonstrating that overexpression of these proteins increases NE budding in more mature primary neuronal cultures, further highlighting a critical role for developmental timing in torsin protein family function emphasized by our *in vivo* studies. The finding that torsinB can effect rescue is critical, because any therapeutic strategy based on increasing endogenous torsinA levels will necessarily increase DYT1 mutant torsinA – which could negate any beneficial increases from the wild type protein through dominant negative effects. In contrast, modulation of torsinB should overcome this obstacle. Considered together, our observations demonstrate that torsinB is a potent modifier of torsinA phenotypes and a potential therapeutic target. Future studies will be required determine the precise role of torsinB in this process, whether overexpression of torsinB can suppress NE bud formation *in vivo*, and if this will ameliorate the behavioral phenotypes in torsinA mutant mice (Liang et al., 2014; Pappas et al., 2015; Weisheit and Dauer, 2015)

The discrete window during which NE buds form implicates several developmental events as potentially related to this process. One intriguing possibility is that torsin proteins function in interphase nuclear pore insertion, a process that is markedly upregulated in maturing neurons (Lodin et al., 1978). Several yeast strains mutant for nucleoporins develop structures similar to NE buds (Siniossoglou et al., 1996; Wente and Blobel, 1994; Zabel et al., 1996), and torsinA loss-of-function in *C. elegans* causes nuclear pore abnormalities and NE bud-like structures (VanGompel et al., 2015), potentially linking these processes. In the striatum, the period of NE bud formation corresponds to the time that neurons are integrating into circuits, when profound changes in neural physiology occur – including the formation of projections and synapses (Uryu et al., 1999). These events impact the NE by upregulating transcription – visually apparent from the transition from hetero- to euchromatin in maturing neurons – and translation, increasing the need for nucleo-cytosolic transport to deliver mRNAs to the cytosol. Transcription and translation are associated with an increase in nuclear pore number in interphase cells (Doucet and Hetzer, 2010; Maul et al., 1980). In the CNS, the number of nuclear pores increases dramatically during cortical neuron maturation (roughly five-fold; (Lodin et al., 1978), and following increased synaptic activity (Wittmann et al., 2009). Synaptic activity increases nuclear membrane surface area as well as nuclear pore number, a form of structural plasticity that may reflect adaptation to a metabolically more active state (Wittmann et al., 2009). Increasing nuclear membrane surface area and related neurodevelopmental events (e.g., process formation) require membrane synthesis. TorsinA has been linked to lipid metabolism (Grillet, et al., 2016) and several observations in yeast demonstrate that disruption of phospolipid and related pathways can cause NE

abnormalities–some of which resemble NE buds (Schneiter et al., 1996; Siniossoglou, 2009). Finally, a series of observations suggests the presence of a nuclear pore-independent form of nucleo-cytosolic transport at specific developmental stages and at times of high metabolic demand (Speese et al., 2012). This process appears to transport large ribonuclear particles directly through the membrane in a manner akin to herpesvirus budding (Speese et al., 2012), but likely differs in important respects since herpesvirus budding proceeds normally in the absence of torsin proteins (Turner et al., 2015). TorsinA, a membrane associated protein, may participate in any of these processes, which are likely strongly upregulated in maturing neurons.

Our findings fundamentally advance understanding of torsinA-related NE budding, linking this process to a discrete neurodevelopmental window, and identify the developmental expression pattern of torsinB as a molecular mechanism governing the temporal window of neural susceptibility to torsinA loss-of-function. The importance of this process for dystonia pathogenesis is supported by the presence of NE budding in LAP1 null mice and the recent connection of LAP1 to human dystonia (Dorboz et al., 2014). Our development of an *in vitro* system modeling this phenomenon, and the demonstration that NE budding can be rescued by torsinB, establish a powerful platform to further dissect this biological process.

Supplementary Material

Refer to Web version on PubMed Central for supplementary material.

Acknowledgments

We thank Roger Albin and members of the Dauer lab for their careful reading of and suggestions for this manuscript. We also thank Rose Goodchild and Christian Schlieker for the kind gift of antibodies to torsinB and Christian Schlieker for antibodies to LAP1 and LULL1. This research project was supported in part by Bachmann-Strauss Dystonia and Parkinson Disease Foundation, a Fellowship from the Dystonia Medical Research Foundation (to L.M. Tanabe), the Robert P. Apkarian Integrated Electron Microscopy Core of Emory University, and a grant from the National Institute of Neurological Disorders and Stroke (1R01NS077730 to W.T. Dauer).

References

Bahn E, Siegert S, Pfander T, Kramer ML, Schulz-Schaeffer WJ, Hewett JW, Breakefield XO, Hedreen JC, Rostásy KM. TorsinB expression in the developing human brain. Brain Res. 2006; 1116:112–119. DOI: 10.1016/j.brainres.2006.07.102 [PubMed: 16938275]

Bain G, Ray WJ, Yao M, Gottlieb DI. Retinoic acid promotes neural and represses mesodermal gene expression in mouse embryonic stem cells in culture. Biochem Biophys Res Commun. 1996; 223:691–694. DOI: 10.1006/bbrc.1996.0957 [PubMed: 8687458]

Brown RSH, Zhao C, Chase AR, Wang J, Schlieker C. The mechanism of Torsin ATPase activation. Proc Natl Acad Sci USA. 2014; 111:E4822–31. DOI: 10.1073/pnas.1415271111 [PubMed: 25352667]

Burke RE, Fahn S, Gold AP. Delayed-onset dystonia in patients with “static” encephalopathy. J Neurol Neurosurg Psychiatr. 1980; 43:789–797. [PubMed: 7191439]

CLARK WH. Electron microscope studies of nuclear extrusions in pancreatic acinar cells of the rat. J Biophys Biochem Cytol. 1960; 7:345–352. [PubMed: 13810485]

Connors SL, Levitt P, Matthews SG, Slotkin TA, Johnston MV, Kinney HC, Johnson WG, Dailey RM, Zimmerman AW. Fetal mechanisms in neurodevelopmental disorders. Pediatr Neurol. 2008; 38:163–176. DOI: 10.1016/j.pediatrneurol.2007.10.009 [PubMed: 18279750]

Dorboz I, Coutelier M, Bertrand AT, Caberg JH, Elmaleh-Bergès M, Lainé J, Stevanin G, Bonne G, Boespflug-Tanguy O, Servais L. Severe dystonia, cerebellar atrophy, and cardiomyopathy likely caused by a missense mutation in TOR1AIP1. Orphanet J Rare Dis. 2014; 9:174.doi: 10.1186/s13023-014-0174-9 [PubMed: 25425325]

Doucet CM, Hetzer MW. Nuclear pore biogenesis into an intact nuclear envelope. Chromosoma. 2010; 119:469–477. DOI: 10.1007/s00412-010-0289-2 [PubMed: 20721671]

GAY H. Nucleocytoplasmic relations in Drosophila. Cold Spring Harb Symp Quant Biol. 1956; 21:257–269. [PubMed: 13433596]

Gonzalez-Alegre P, Paulson HL. Aberrant cellular behavior of mutant torsinA implicates nuclear envelope dysfunction in DYT1 dystonia. J Neurosci. 2004; 24:2593–2601. DOI: 10.1523/JNEUROSCI.4461-03.2004 [PubMed: 15028751]

Goodchild RE, Dauer WT. Mislocalization to the nuclear envelope: an effect of the dystonia-causing torsinA mutation. Proc Natl Acad Sci USA. 2004; 101:847–852. DOI: 10.1073/pnas.0304375101 [PubMed: 14711988]

Goodchild RE, Kim CE, Dauer WT. Loss of the dystonia-associated protein torsinA selectively disrupts the neuronal nuclear envelope. Neuron. 2005; 48:923–932. DOI: 10.1016/j.neuron.2005.11.010 [PubMed: 16364897]

Grillet M, Dominguez Gonzalez B, Sicart A, Pöttler M, Cascalho A, Billion K, Hernandez Diaz S, Swerts J, Naismith T, Gounko N, Verstreken P, Hanson P, Goodchild R. Torsins Are Essential Regulators of Cellular Lipid Metabolism. Developmental Cell. 2016; 38:1–13. [PubMed: 27404350]

Hadek R, Swift H. Nuclear extrusion and intracisternal inclusions in the rabbit blastocyst. J Cell Biol. 1962; 13:445–451. [PubMed: 13903455]

Hochstrasser M, Sedat JW. Three-dimensional organization of Drosophila melanogaster interphase nuclei. II Chromosome spatial organization and gene regulation. J Cell Biol. 1987a; 104:1471–1483. [PubMed: 3108265]

Hochstrasser M, Sedat JW. Three-dimensional organization of Drosophila melanogaster interphase nuclei. I Tissue-specific aspects of polytene nuclear architecture. J Cell Biol. 1987b; 104:1455–1470. [PubMed: 3108264]

Hoftman GD, Lewis DA. Postnatal developmental trajectories of neural circuits in the primate prefrontal cortex: identifying sensitive periods for vulnerability to schizophrenia. Schizophr Bull. 2011; 37:493–503. DOI: 10.1093/schbul/sbr029 [PubMed: 21505116]

Jokhi V, Ashley J, Nunnari J, Noma A, Ito N, Wakabayashi-Ito N, Moore MJ, Budnik V. Torsin mediates primary envelopment of large ribonucleoprotein granules at the nuclear envelope. Cell Rep. 2013; 3:988–995. DOI: 10.1016/j.celrep.2013.03.015 [PubMed: 23583177]

Jungwirth M, Dear ML, Brown P, Holbrook K, Goodchild R. Relative tissue expression of homologous torsinB correlates with the neuronal specific importance of DYT1 dystonia-associated torsinA. Hum Mol Genet. 2010; 19:888–900. DOI: 10.1093/hmg/ddp557 [PubMed: 20015956]

Jungwirth MT, Kumar D, Jeong DY, Goodchild RE. The nuclear envelope localization of DYT1 dystonia torsinA-ΔE requires the SUN1 LINC complex component. BMC Cell Biol. 2011; 12:24.doi: 10.1186/1471-2121-12-24 [PubMed: 21627841]

Kim CE, Perez A, Perkins G, Ellisman MH, Dauer WT. A molecular mechanism underlying the neural-specific defect in torsinA mutant mice. Proc Natl Acad Sci USA. 2010; 107:9861–9866. DOI: 10.1073/pnas.0912877107 [PubMed: 20457914]

Liang CC, Tanabe LM, Jou S, Chi F, Dauer WT. TorsinA hypofunction causes abnormal twisting movements and sensorimotor circuit neurodegeneration. J Clin Invest. 2014; 124:3080–3092. DOI: 10.1172/JCI72830 [PubMed: 24937429]

Lodin Z, Blumajer J, Mares V. Nuclear pore complexes in cells of the developing mouse cerebral cortex. Acta Histochem. 1978; 63:74–79. DOI: 10.1016/S0065-1281(78)80009-9 [PubMed: 105558]

Machold R, Fishell G. Math1 is expressed in temporally discrete pools of cerebellar rhombic-lip neural progenitors. Neuron. 2005; 48:17–24. DOI: 10.1016/j.neuron.2005.08.028 [PubMed: 16202705]

Maric M, Haugo AC, Dauer W, Johnson D, Roller RJ. Nuclear envelope breakdown induced by herpes simplex virus type 1 involves the activity of viral fusion proteins. Virology. 2014; 460–461:128–137. DOI: 10.1016/j.virol.2014.05.010

Maul GG, Deaven LL, Freed JJ, Campbell GL, Beçak W. Investigation of the determinants of nuclear pore number. Cytogenet Cell Genet. 1980; 26:175–190. [PubMed: 6966999]

Mizuhara E, Minaki Y, Nakatani T, Kumai M, Inoue T, Muguruma K, Sasai Y, Ono Y. Purkinje cells originate from cerebellar ventricular zone progenitors positive for Neph3 and E-cadherin. Dev Biol. 2010; 338:202–214. DOI: 10.1016/j.ydbio.2009.11.032 [PubMed: 20004188]

Monory K, Massa F, Egertová M, Eder M, Blaudzun H, Westenbroek R, Kelsch W, Jacob W, Marsch R, Ekker M, Long J, Rubenstein JL, Goebbels S, Nave KA, During M, Klugmann M, Wölfel B, Dodt HU, Zieglgänsberger W, Wotjak CT, Mackie K, Elphick MR, Marsicano G, Lutz B. The endocannabinoid system controls key epileptogenic circuits in the hippocampus. Neuron. 2006; 51:455–466. DOI: 10.1016/j.neuron.2006.07.006 [PubMed: 16908411]

Naismith TV, Dalal S, Hanson PI. Interaction of torsinA with its major binding partners is impaired by the dystonia-associated DeltaGAG deletion. J Biol Chem. 2009; 284:27866–27874. DOI: 10.1074/jbc.M109.020164 [PubMed: 19651773]

Naismith TV, Heuser JE, Breakefield XO, Hanson PI. TorsinA in the nuclear envelope. Proc Natl Acad Sci USA. 2004; 101:7612–7617. DOI: 10.1073/pnas.0308760101 [PubMed: 15136718]

Nery FC, Zeng J, Niland BP, Hewett J, Farley J, Irimia D, Li Y, Wiche G, Sonnenberg A, Breakefield XO. TorsinA binds the KASH domain of nesprins and participates in linkage between nuclear envelope and cytoskeleton. J Cell Sci. 2008; 121:3476–3486. DOI: 10.1242/jcs.029454 [PubMed: 18827015]

Novitch BG, Chen AI, Jessell TM. Coordinate regulation of motor neuron subtype identity and pan-neuronal properties by the bHLH repressor Olig2. Neuron. 2001; 31:773–789. [PubMed: 11567616]

Ozelius LJ, Hewett JW, Page CE, Bressman SB, Kramer PL, Shalish C, de Leon D, Brin MF, Raymond D, Corey DP, Fahn S, Risch NJ, Buckler AJ, Gusella JF, Breakefield XO. The early-onset torsion dystonia gene (DYT1) encodes an ATP-binding protein. Nat Genet. 1997; 17:40–48. DOI: 10.1038/ng0997-40 [PubMed: 9288096]

Pappas SS, Darr K, Holley SM, Cepeda C, Mabrouk OS, Wong JMT, LeWitt TM, Paudel R, Houlden H, Kennedy RT, Levine MS, Dauer WT. Forebrain deletion of the dystonia protein torsinA causes dystonic-like movements and loss of striatal cholinergic neurons. Elife. 2015; 4:e08352.doi: 10.7554/eLife.08352 [PubMed: 26052670]

Schneiter R, Hitomi M, Ivessa AS, Fasch EV, Kohlwein SD, Tartakoff AM. A yeast acetyl coenzyme A carboxylase mutant links very-long-chain fatty acid synthesis to the structure and function of the nuclear membrane-pore complex. Mol Cell Biol. 1996; 16:7161–7172. [PubMed: 8943372]

Shaw P, Gogtay N, Rapoport J. Childhood psychiatric disorders as anomalies in neurodevelopmental trajectories. Hum Brain Mapp. 2010; 31:917–925. DOI: 10.1002/hbm.21028 [PubMed: 20496382]

Siniossoglou S. Lipins, lipids and nuclear envelope structure. Traffic. 2009; 10:1181–1187. DOI: 10.1111/j.1600-0854.2009.00923.x [PubMed: 19490535]

Siniossoglou S, Wimmer C, Rieger M, Doye V, Tekotte H, Weise C, Emig S, Segref A, Hurt EC. A novel complex of nucleoporins, which includes Sec13p and a Sec13p homolog, is essential for normal nuclear pores. Cell. 1996; 84:265–275. [PubMed: 8565072]

Soriano P. Generalized lacZ expression with the ROSA26 Cre reporter strain. Nat Genet. 1999; 21:70–71. DOI: 10.1038/5007 [PubMed: 9916792]

Sosa BA, Demircioglu FE, Chen JZ, Ingram J, Ploegh HL, Schwartz TU. How lamina-associated polypeptide 1 (LAP1) activates Torsin. Elife. 2014; 3:e03239.doi: 10.7554/eLife.03239 [PubMed: 25149450]

Speese SD, Ashley J, Jokhi V, Nunnari J, Barria R, Li Y, Ataman B, Koon A, Chang YT, Li Q, Moore MJ, Budnik V. Nuclear envelope budding enables large ribonucleoprotein particle export during synaptic Wnt signaling. Cell. 2012; 149:832–846. DOI: 10.1016/j.cell.2012.03.032 [PubMed: 22579286]

Strambio-De-Castilla C. Jumping over the fence: RNA nuclear export revisited. Nucleus. 2013; 4:95–99. DOI: 10.4161/nucl.24237 [PubMed: 23528257]

Szöllösi D. Extrusion of nucleoli from pronuclei of the rat. J Cell Biol. 1965; 25:545–562. [PubMed: 5320297]

Szöllösi MS, Szöllösi D. “Blebbing” of the nuclear envelope of mouse zygotes, early embryos and hybrid cells. J Cell Sci. 1988; 91(Pt 2):257–267. [PubMed: 3267698]

Tanabe LM, Martin C, Dauer WT. Genetic background modulates the phenotype of a mouse model of DYT1 dystonia. PLoS ONE. 2012; 7:e32245.doi: 10.1371/journal.pone.0032245 [PubMed: 22393392]

Turner EM, Brown RSH, Laudermilch E, Tsai PL, Schlieker C. The Torsin Activator LULL1 Is Required for Efficient Growth of Herpes Simplex Virus 1. J Virol. 2015; 89:8444–8452. DOI: 10.1128/JVI.01143-15 [PubMed: 26041288]

Uryu K, Butler AK, Chesselet MF. Synaptogenesis and ultrastructural localization of the polysialylated neural cell adhesion molecule in the developing striatum. J Comp Neurol. 1999; 405:216–232. DOI: 10.1002/(SICI)1096-9861(19990308)405:2<216::AID-CNE6>3.0.CO;2-6 [PubMed: 10023811]

VanGompel MJW, Nguyen KCQ, Hall DH, Dauer WT, Rose LS. A novel function for the Caenorhabditis elegans torsin OOC-5 in nucleoporin localization and nuclear import. Mol Biol Cell. 2015; 26:1752–1763. DOI: 10.1091/mbc.E14-07-1239 [PubMed: 25739455]

Vasudevan A, Breakefield XO, Bhide PG. Developmental patterns of torsinA and torsinB expression. Brain Res. 2006; 1073–1074:139–145. DOI: 10.1016/j.brainres.2005.12.087

Weisheit CE, Dauer WT. A novel conditional knock-in approach defines molecular and circuit effects of the DYT1 dystonia mutation. Hum Mol Genet. 2015; 24:6459–6472. DOI: 10.1093/hmg/ddv355 [PubMed: 26370418]

Wente SR, Blobel G. NUP145 encodes a novel yeast glycine-leucine-phenylalanine-glycine (GLFG) nucleoporin required for nuclear envelope structure. J Cell Biol. 1994; 125:955–969. [PubMed: 8195299]

Wittmann M, Queisser G, Eder A, Wiegert JS, Bengtson CP, Hellwig A, Wittum G, Bading H. Synaptic activity induces dramatic changes in the geometry of the cell nucleus: interplay between nuclear structure, histone H3 phosphorylation, and nuclear calcium signaling. J Neurosci. 2009; 29:14687–14700. doi:10.1523.J.Neurosci.1160-09.2009. [PubMed: 19940164]

Zabel U, Doye V, Tekotte H, Wepf R, Grandi P, Hurt EC. Nic96p is required for nuclear pore formation and functionally interacts with a novel nucleoporin, Nup188p. J Cell Biol. 1996; 133:1141–1152. [PubMed: 8682854]

Zhao C, Brown RSH, Chase AR, Eisele MR, Schlieker C. Regulation of Torsin ATPases by LAP1 and LULL1. Proc Natl Acad Sci USA. 2013; 110:E1545–54. DOI: 10.1073/pnas.1300676110 [PubMed: 23569223]

Zhu Y, Romero MI, Ghosh P, Ye Z, Charnay P, Rushing EJ, Marth JD, Parada LF. Ablation of NF1 function in neurons induces abnormal development of cerebral cortex and reactive gliosis in the brain. Genes Dev. 2001; 15:859–876. DOI: 10.1101/gad.862101 [PubMed: 11297510]

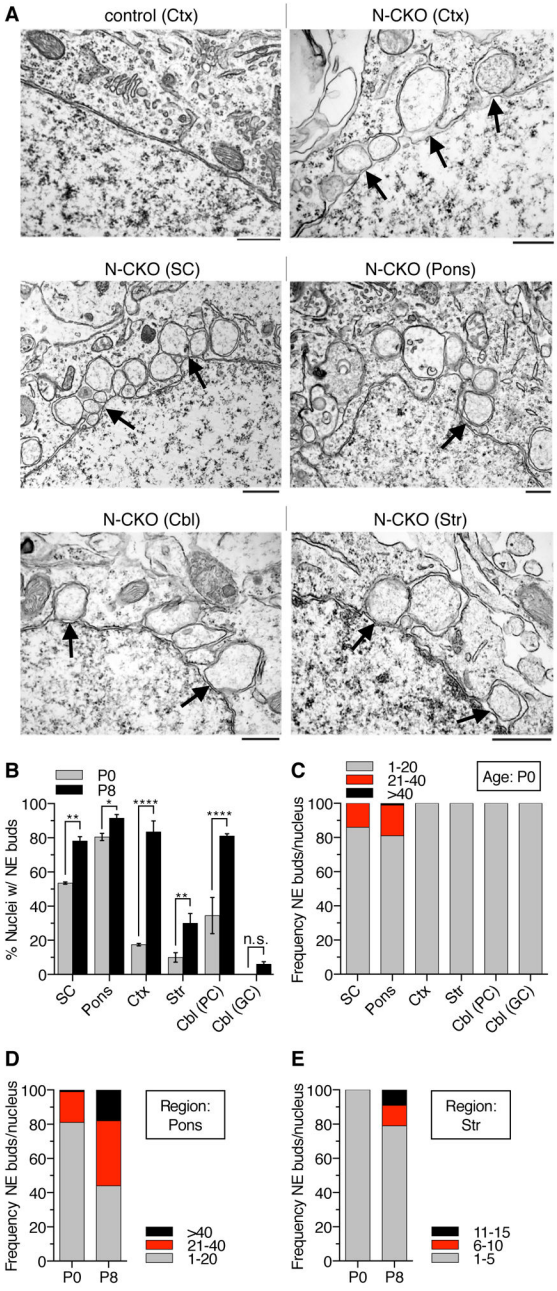

Figure 1. Neuronal Nuclear Membrane Budding Increases During Early Postnatal CNS Maturation

Conditional CNS deletion of torsinA caused neuronal NE buds in all CNS regions examined. (A) Ultrastructural images of normal control and nestin-*Cre* conditional knockout (N-CKO) neuronal nuclei with NE budding from P8 cortex (ctx; first row). Subsequent rows are examples from spinal cord (SC), pons, Purkinje cells of cerebellum (Cbl), and striatum (Str). Nuclear membrane buds are denoted by arrows, N = Nucleus, C = Cytosol. Scale bar = 500 nm. (B) Percentage of nuclei with NE buds in the CNS regions shown in (A) at P0 and P8 (n = 2, per region/age). PC = Purkinje cells; GC = granule cells. Results are expressed as mean ± SEM. One-way Anova; * = $P < 0.05$, ** = $P < 0.01$, **** = $P < 0.0001$. (C) Stacked bar

graphs showing percentage of nuclei (at P0) with different numbers of buds/nucleus by region in all regions examined. (D–E) The number of NE buds/nucleus continues to accumulate from P0 to P8. Stacked bar graphs show percentage of nuclei with different numbers of buds/nucleus in (D) pons and (E) striatum (n = 2, per region/age).

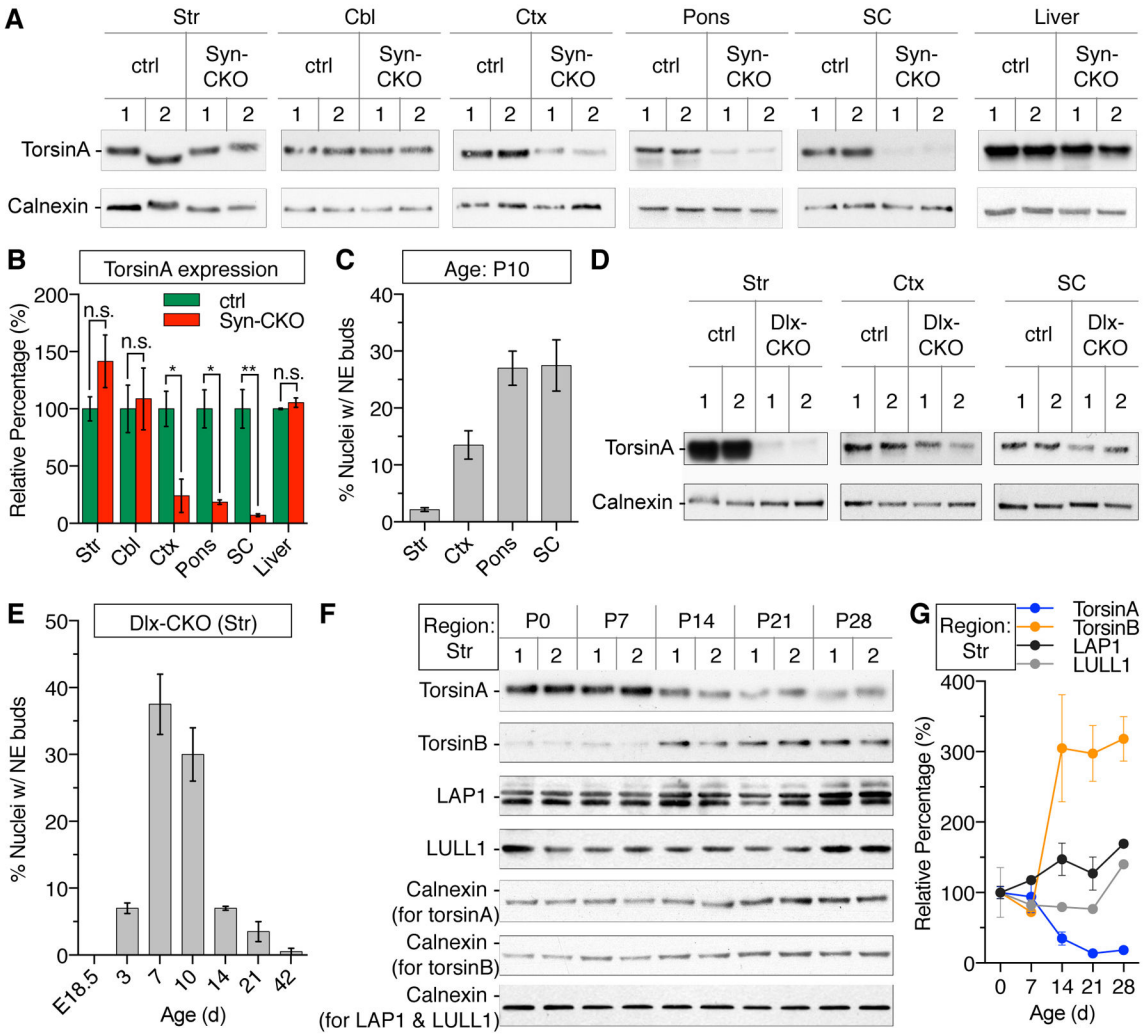

Figure 2. Neuronal Nuclear Membrane Budding is a Cell Autonomous Process that Occurs During a Neurodevelopmental Window

(A) Western blot demonstrating efficient deletion of torsinA protein in Syn-CKO mice in cortex (Ctx), pons, and spinal cord (SC), but not striatum (Str), cerebellum (Cbl), or liver (n = 2, per region). (B) Quantification of the torsinA western blots displayed in (A). (C) Percentage of nuclei with NE buds in P10 Syn-CKO mice in regions of confirmed torsinA deletion. Results are expressed as mean ± SEM. (D) Western blot showing efficient deletion of torsinA protein from striatum in Dlx-CKO mice. (E) Developmental time course of NE bud frequency in striatum of Dlx-CKO mice from E18.5 to P42 reveals the trajectory of NE bud development, peak, and resolution. (F) Striatal lysates from wild-type mice demonstrate that endogenous levels of torsinB levels are low as NE buds accumulate (P0 to P7), and that torsinA and torsin B exhibit opposite changes in levels of expression as NE buds resolve (P7 to P28). Levels of the torsinA-interacting proteins LAP1 and LULL1 remain largely unchanged during this period of CNS maturation. The changes for torsinA, torsinB, LAP1, and LULL1 are quantified in (G) as a relative percentage to calnexin control. Results are expressed as mean ± SEM. All lysates in duplicate for western blot.

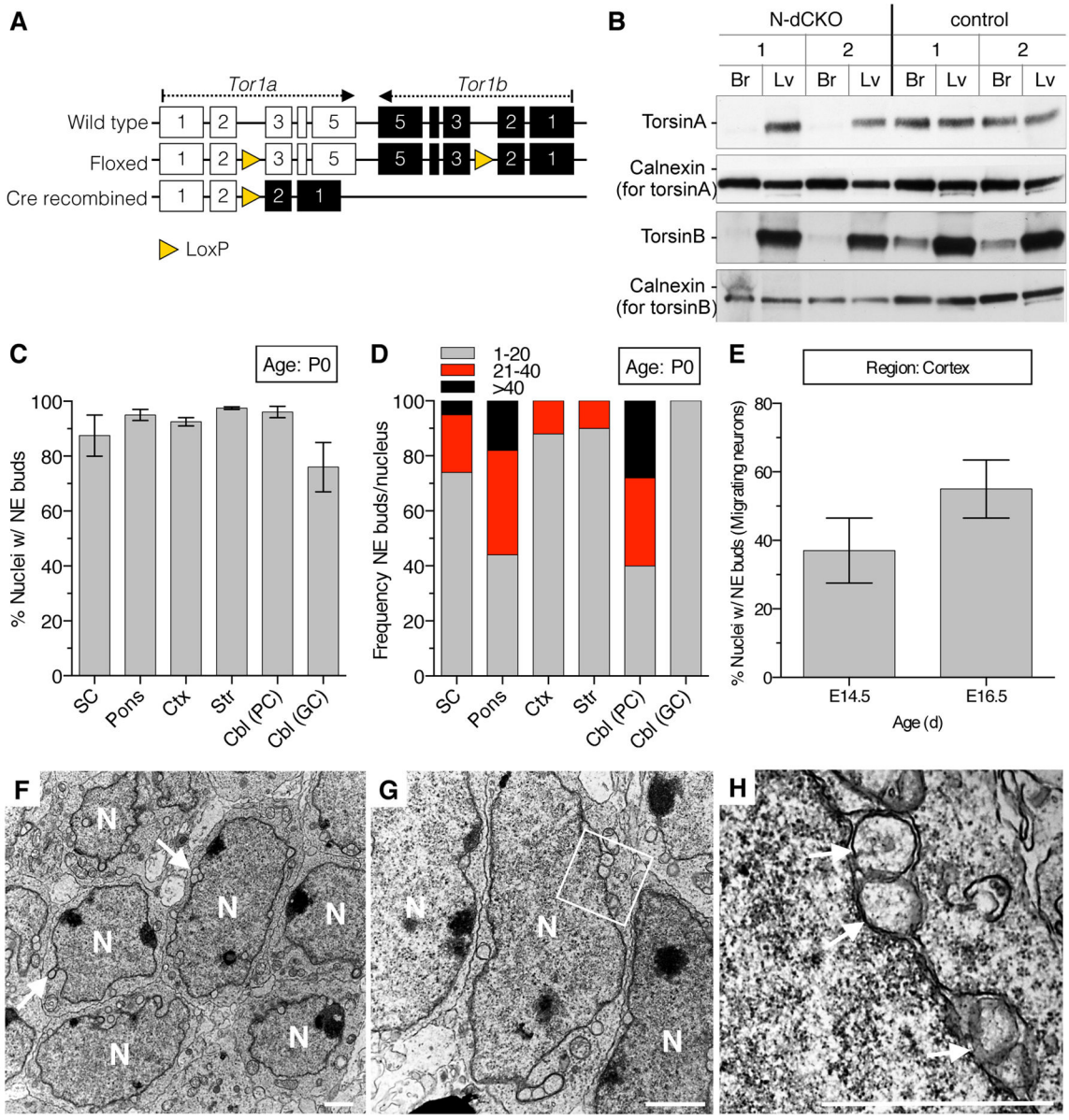

Figure 3. TorsinB Modulates the Timing of Critical Period Opening for Neuronal NE Budding

(A) Schematic of the floxed *Tor1(ab)* allele and product of Cre recombination. (B) Western blot demonstrating deletion of torsinA and torsinB from brain (Br), but not liver (Lv) in N-dCKO mice. (C) Neurons of N-dCKO mice exhibit similarly high levels NE bud formation in areas of differing developmental age/maturational state (P0; n = 2, per region/age). (D) Stacked bar graphs show percentage of nuclei with differing numbers of buds/nucleus by region (P0). (E) N-dCKO mice exhibit NE budding in migrating cortical neurons, a developmental stage in which budding does not occur in N-CKO mice. Quantification of percentage of affected nuclei (n = 2 per age). (F – H) Ultrastructural images of migrating cortical neurons of N-dCKO animals at E16.5. (F) Low magnification image of several migrating nuclei (N). (G) Higher magnification of elongated migrating nuclei with NE buds.

(H) Boxed NE from (G) shows arrows pointing at NE buds at greater magnification. Scale bars = 1 um. Results are expressed as mean ± SEM.

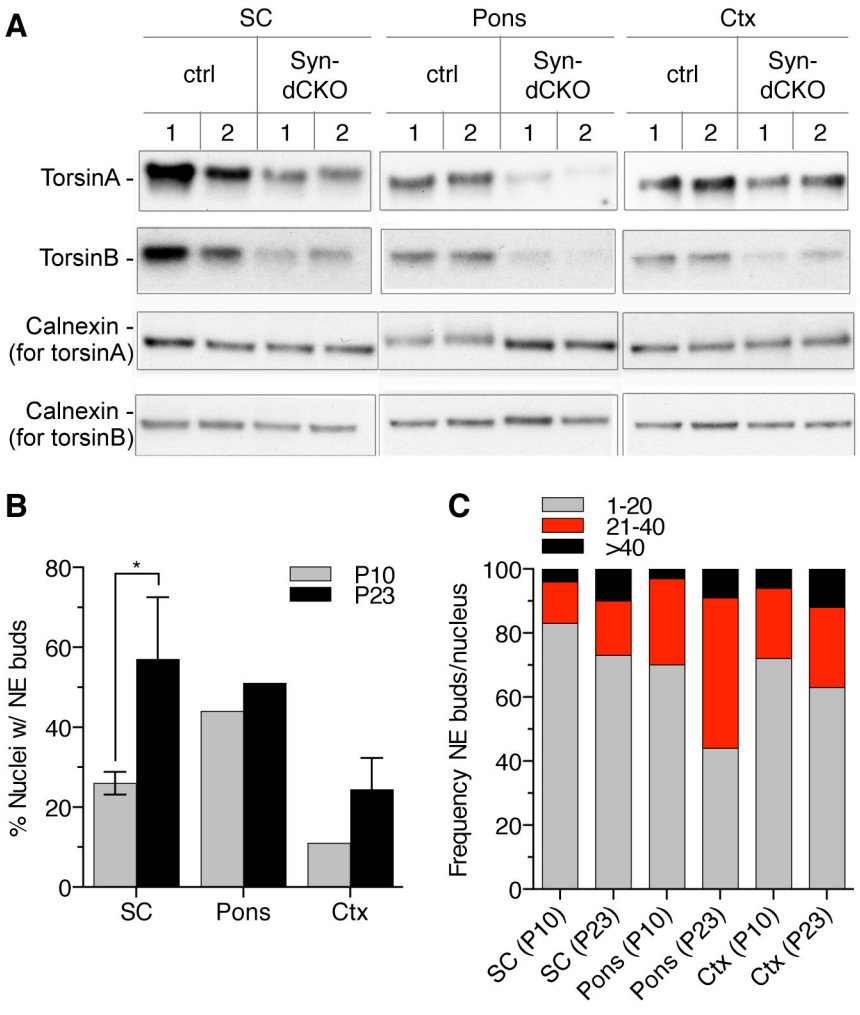

Figure 4. TorsinB Modulates the Timing of Neurodevelopmental Window Closure for NE Budding

(A) Western blot demonstrating conditional deletion of torsinA and torsinB protein in spinal cord (SC), pons, and cortex (Ctx) in Syn-dCKO mice. Note that Synapsin 1-*Cre* expresses exclusively within neurons, so much of the remaining protein likely derives from non-neuronal cells. (B) NE budding continues to increase in Syn-dCKO neurons from P10 to P23, when it resolves completely in Syn-CKO mice (n = 2, per region/age). One-way Anova; * = $P < 0.05$. (C) Stacked bar graph shows percentage of nuclei with differing numbers of buds/nucleus (P10 and P23). Note that NE buds/nucleus continues to accumulate during this time. Results are expressed as mean ± SEM.

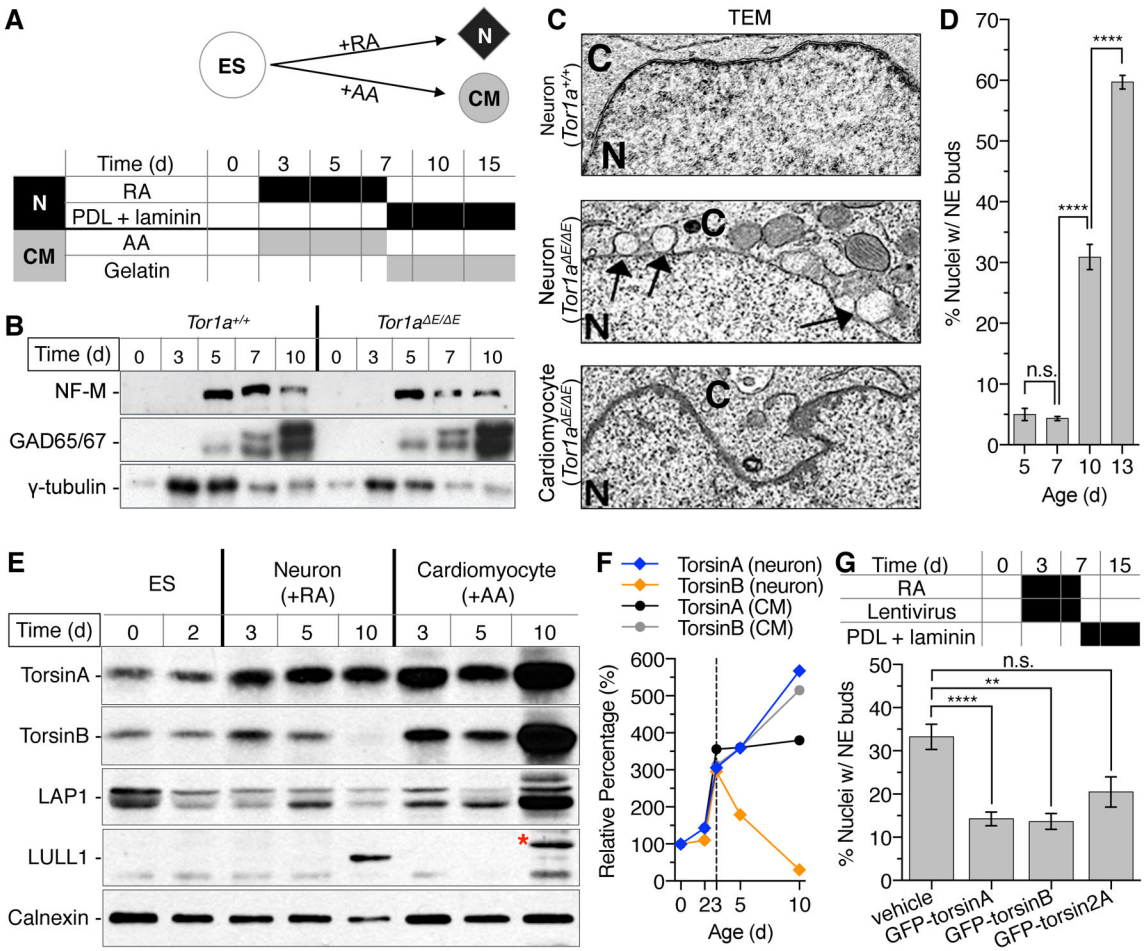

Figure 5. TorsinB overexpression suppresses NE budding during the maturation of DYT1-mutant neurons

(A) Diagrammatic overview of experimental design. Wild-type and DYT1-mutant mouse ES (mES) cells were grown in suspension for 2 days to form embryoid bodies (EBs). They were then driven down either a neural or cardiomyocyte lineage. For the neural lineage, they were exposed to retinoic acid (RA) for 5 days and subsequently plated on poly-D-lysine (PDL) and laminin for up to 8 days, during which time they extended processes, and neuron (N) markers. For the cardiomyocyte (CM) lineage, they were exposed to ascorbic acid (AA) for 5 days and subsequently plated on gelatin for up to 8 days; these cultures developed beating foci within 48 hours of AA exposure. (B) Western blots of NF-M and GAD65/67 demonstrating that control and DYT1-mutant mES cells differentiate into neurons with a similar time course following RA exposure. γ-tubulin used as loading control. (C) Ultrastructural analysis of mutant neurons and muscle demonstrates the development of NE buds selectively in the neural lineage that are indistinguishable from those observed in mouse brain. (D) Percentage of neuronal nuclei with buds increases as the cells mature on PDL/laminin (n = 2 per time-point). (E) Expression of torsinA, torsinB, LAP1 and LULL1 demonstrates a unique divergence of torsinB expression levels during neural and cardiomyocyte differentiation. Note that the asterisk denotes the major immunoreactive band of LULL1 in the cardiomyocyte lysate. (F) Relative quantification of torsinA and torsinB

levels shown in (E). (G) Introduction of lentiviral GFP-torsinA, GFP-torsinB, or GFP-torsin2A midway through neuronal differentiation. Both torsinA and torsinB rescued NE budding phenotype in mutant neuronal EBs. Mann-Whitney: Compared to vehicle, GFP-torsinA: P = 0.000094; GFP-torsinB: P = 0.006365 ; P = 0.112278; ** = P < 0.01,**** = P < 0.0001. Results are expressed as mean ± SEM.